

11-44-89
J52016
40P.

JPL Publication 89-47

Results of the 1989 NASA/JPL Balloon Flight Solar Cell Calibration Program

B. E. Anspaugh
R. S. Weiss

November 15, 1989



National Aeronautics and
Space Administration

Jet Propulsion Laboratory
California Institute of Technology
Pasadena, California

(NASA-CR-186114) RESULTS OF THE 1989
NASA/JPL BALLOON FLIGHT SOLAR CELL
CALIBRATION PROGRAM (JPL) 40 p CSCL 10A

N90-14672

Unclas
G3/44 0252016

12/12/2020

JPL Publication 89-47

Results of the 1989 NASA/JPL Balloon Flight Solar Cell Calibration Program

B. E. Anspaugh
R. S. Weiss

November 15, 1989

NASA

National Aeronautics and
Space Administration

Jet Propulsion Laboratory
California Institute of Technology
Pasadena, California

The research described in this publication was carried out by the Jet Propulsion Laboratory, California Institute of Technology, under a contract with the National Aeronautics and Space Administration.

Reference herein to any specific commercial product, process, or service by trade name, trademark, manufacturer, or otherwise, does not constitute or imply its endorsement by the United States Government or the Jet Propulsion Laboratory, California Institute of Technology.

ABSTRACT

The 1989 solar cell calibration balloon flight was successfully completed on August 9, 1989, meeting all objectives of the program. Forty-two modules were carried to an altitude of 118,000 ft (36.0 km). The calibrated cells can now be used as reference standards in simulator testing of cells and arrays.

ACKNOWLEDGMENT

The authors wish to extend appreciation for the cooperation and support provided by the entire staff of the National Scientific Balloon Facility located in Palestine, Texas. The cooperation and patience extended by all participating organizations are greatly appreciated.

CONTENTS

1. INTRODUCTION AND OVERVIEW	1
2. PREFLIGHT PROCEDURES	3
2.1 MODULE FABRICATION	3
2.2 CELL MEASUREMENTS	3
2.3 TEMPERATURE COEFFICIENTS AND LEAST SQUARES FITS	4
2.4 PANEL ASSEMBLY AND CHECKOUT	4
2.5 PRELAUNCH PROCEDURES AT PALESTINE	7
3. BALLOON SYSTEM	8
3.1 BALLOON DESCRIPTION	8
3.2 TOP PAYLOAD	10
3.3 BOTTOM PAYLOAD	13
4. FLIGHT SEQUENCE	17
4.1 PRELAUNCH PREPARATIONS	17
4.2 FLIGHT	21
4.3 FLIGHT TERMINATION	22
5. DATA ANALYSIS	25
5.1 COMPUTER ANALYSIS	25
5.2 CALIBRATION RESULTS	28
5.3 UPDATE OF BFS-17A DATA	28
6. CONCLUSIONS	32
7. REFERENCE	33

Figures

Figure 1.	Photograph of the 1989 Balloon Flight Solar Panel	5
Figure 2.	1989 Module Location Chart	6
Figure 3.	Aluminum Hoop Assembly with Tracker Mounted	9
Figure 4.	Block Diagram of Balloon Telemetry System	14
Figure 5.	Flight Train Configuration	19
Figure 6.	Balloon Launch	20
Figure 7.	1989 Balloon Flight Profile	24

Tables

Table 1.	1989 Balloon Flight 8/9/89 118,000 ft RV=1.0136862	
	Flight No. 1486P	30
Table 2.	Repeatability of Standard Solar Cell BFS-17A	31

1. INTRODUCTION AND OVERVIEW

The primary source of electrical power for unmanned space vehicles is the direct conversion of solar energy through the use of solar cells. As advancing cell technology continues to modify the spectral response of solar cells to utilize more of the sun's spectrum, designers of solar cells and arrays must have the capability of measuring these cells in a light beam that is a close match to the solar spectrum. The solar spectrum has been matched very closely by laboratory solar simulators. But the design of solar cells and the sizing of solar arrays require such highly accurate measurements that the intensity of these simulators must be set very accurately. A small error in setting the simulator intensity can conceivably cause a disastrous mis-sizing of a solar panel, causing either a premature shortfall in power or the launch of an oversized, overweight solar panel.

The JPL solar cell calibration program was conceived to produce reference standards for the purpose of properly setting solar simulator intensities. The concept was to fly solar cells on a high-altitude balloon, measure their output at altitudes near 120,000 ft, recover the cells, and use them as reference standards. The procedure is simple. The reference cell is placed in the simulator beam and the beam intensity is adjusted until the reference cell reads the same as it read on the balloon. As long as the reference cell has the same spectral response as the cells or panels to be measured, this is a very accurate method of setting the intensity. But as solar cell technology changes, the spectral response of the solar cells changes also, and reference standards must be continually renewed.

Until the summer of 1985, there had always been a question as to how much the atmosphere above the balloon modified the solar spectrum. If the modification was significant, the reference cells might not have the required accuracy. Solar cells made in recent years have increasingly higher blue responses and if the atmosphere has any effect at all, it would be expected to modify the calibration of these newer blue cells much more so than for cells made in the past.

In late 1984, a collection of solar cells representing a wide cross section of solar cell technology was flown on the shuttle Discovery as a part of the Solar Cell Calibration Facility (SCCF) experiment. The cells were calibrated as reference cells on this flight using procedures similar to those used on the balloon flights. The same cells were then flown on the 1985 balloon flight and remeasured. Since the two sets of measurements gave nearly identical results (See Ref.), the reference standards from balloon flights may continue to be used with high confidence.

2. PREFLIGHT PROCEDURES

2.1 MODULE FABRICATION

The cells were mounted by the participants on JPL-supplied standard modules according to standard procedures developed for the construction of reference cells. The JPL standard module is a machined copper block, rimmed by a fiberglass circuit board with insulated solder posts. This assembly is painted with either high-reflectance white or low-reflectance black paint and is permanently provided with a load resistor. The resistor performs two tasks. First, it loads the cells near short-circuit current, which is the cell parameter that varies in direct proportion to light intensity. Second, it scales the cell outputs to read near 100 mV during the flight, matching a constraint imposed by the telemetry electronics. Load resistance values are 0.5 ohm for a 2 x 2 cm cell, 0.25 ohm for a 2 x 4 cm cell, etc. The load resistors are precision (0.1 percent, 20 ppm/°C) and have a resistance stability equal to or better than $\pm 0.002\%$ over a three-year period.

The 1989 flight incorporated 42 solar cell modules from 11 different vendors. The cells included Si, GaAs, InP, CuInSe₂, and several tandem cells incorporating cell stacks of various kinds. JPL Module BFS-17A was included again, as it has been on every balloon flight since 1963. Its output continues to update our historical record of the calibration procedure repeatability.

2.2 CELL MEASUREMENTS

After the cells were mounted onto the copper blocks, the electrical output of each cell module was measured under illumination by the JPL X25 Mark II solar simulator. For these measurements, the simulator

intensity was set using only one reference cell--no attempt was made to match the spectral response of the reference standard to the individual cell modules. The absolute accuracy of these measurements is therefore unknown, but the measurements do allow checking of the modules for any unacceptable assembly losses or instabilities. After the balloon flight, the cells were measured in exactly the same way to check for any cell damage or instabilities that may have occurred as a result of the flight.

2.3 TEMPERATURE COEFFICIENTS AND LEAST SQUARES FITS

The temperature coefficients of the mounted cells were also measured before the flight. The modules were mounted in their flight configuration on a temperature controlled block in a vacuum chamber. Outputs were measured at 0, 20, 40, 60, and 80° C under illumination with the X25 simulator. The temperature coefficients of the cell modules were computed by fitting the output vs temperature relationship with a linear least squares fit.

2.4 PANEL ASSEMBLY AND CHECKOUT

After the electrical measurements were completed, the modules were mounted on the solar panel and connected electrically. Figure 1 is a photograph of the modules after completion of these steps and Figure 2 is a diagram that identifies the modules in the photograph by their serial numbers. After completion of the panel assembly, the panel and tracker together were given complete functional tests in terrestrial sunlight. The assembled tracker and panel were placed in sunlight on a clear, bright day, and checked for the tracker's ability to acquire and track the sun while each

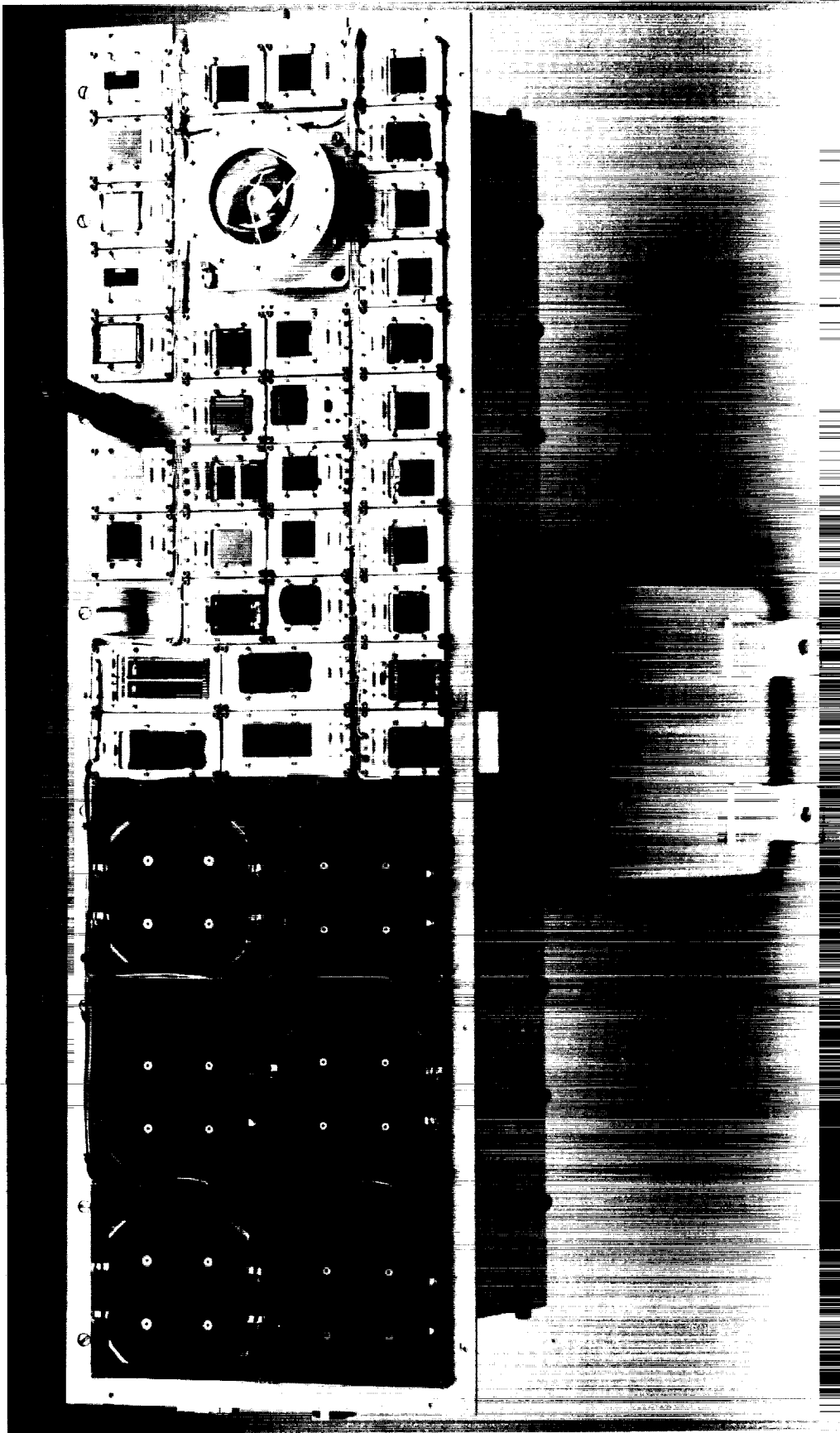
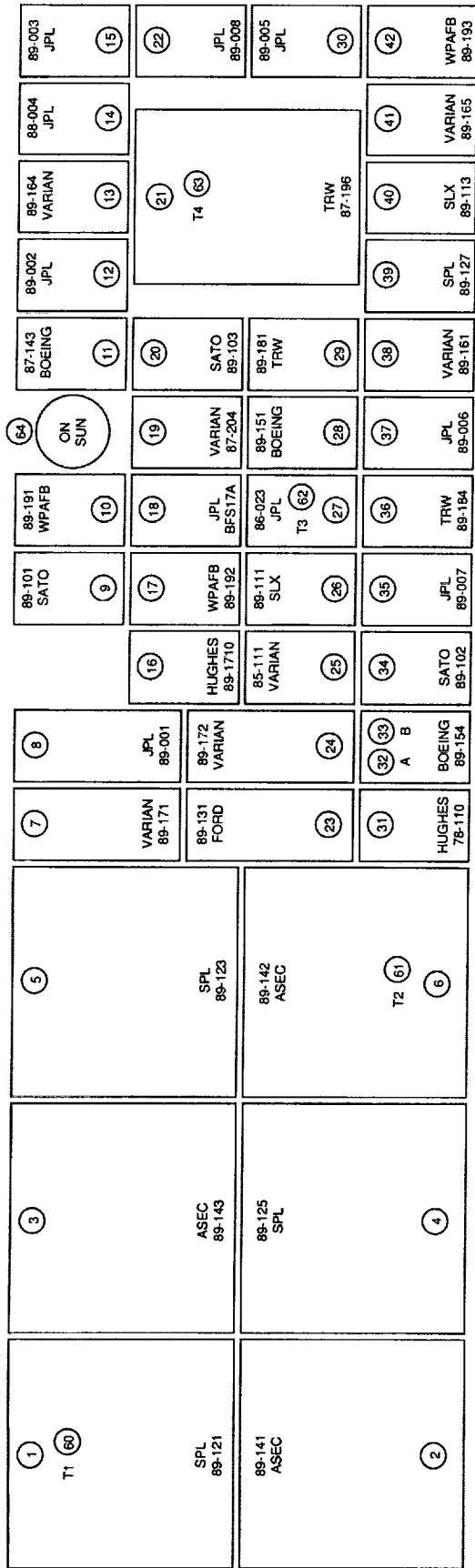


Figure 1. Photograph of the 1989 Balloon Flight Solar Panel



○ INDICATES CHANNEL NUMBER
 T1 (60) THERMISTOR 1
 T2 (61) THERMISTOR 2
 T3 (62) THERMISTOR 3
 T4 (63) THERMISTOR 4

Figure 2. 1989 Module Location Chart

cell module was checked for electrical output. When these tests were completed satisfactorily, the assembly was shipped to the National Scientific Balloon Facility (NSBF) in Palestine, Texas, for flight.

2.5 PRELAUNCH PROCEDURES AT PALESTINE

The NSBF was established in 1963 at Palestine, Texas. This location was chosen because it has favorable weather conditions for balloon launching and a large number of clear days with light surface winds. The high-altitude winds in this part of the country take the balloons over sparsely populated areas so the descending payloads are unlikely to cause damage to persons or property. The JPL calibration flights have flown from the Palestine facility since 1973. The flights are scheduled to fly in July or August, since the sun is high in the sky at that time of year, and the sunlight passes through a minimum depth of atmosphere before reaching the solar modules.

Upon arrival at Palestine, the tracker and module payload were again checked for proper operation. The data encoder was connected to the module payload and an end-to-end check was performed on the payload, telemetry, and receiving and decoding systems. A self-contained voltage reference box was mounted to the tracker assembly and its four output voltage levels were wired into the telemetry stream along with the module outputs. The analog-to-digital converter system was calibrated by recording these four voltage levels as they were input to the system and as they were converted, decoded, and sent through the system as digital output values. The thermistor channels were calibrated by replacing each thermistor, in turn, with a known calibration resistor while the entire system was operating. Eleven resistors are used in this procedure to produce calibrations at 10° increments over the 0 to 100° C

range. The checkout was completed by watching the system over a period of 2 to 3 hours to make sure no stability problems occurred.

After all the checkouts and calibrations were performed, the tracker was mounted onto the aluminum tubular hoop assembly which will ride on the top portion (or apex) of the balloon. Figure 3 is a photograph of the tracker and solar panel after mounting onto the hoop.

3. BALLOON SYSTEM

The main components of the balloon flight system were (1) the apex-mounted hoop assembly that contains the experimental package, the data encoder, the recovery system, and the camera package, (2) the balloon, and (3) the lower payload that contains the telemetry and power systems.

3.1 BALLOON DESCRIPTION

The balloon employed for the JPL solar cell calibration high-altitude flights had a volume of 3.49 million ft^3 ($99,000 \text{ m}^3$) and was made from 0.8-mil (20 micron) stratofilm, a polyethylene film designed for balloon use. The balloon alone weighs 704 pounds (319 kg). The balloon was designed to lift itself, along with the bottom and top payloads, to a float altitude of 120,000 ft (36 km). At float altitude, the balloon will have a diameter of roughly 188 ft (59 m). A multiconductor cable to electrically connect the top and bottom payloads was built into the balloon during its manufacture. The balloon was built with an internal rip line designed to rip a hole in the side of the balloon for termination of the flight. A special structure was built

ORIGINAL PAGE
BLACK AND WHITE PHOTOGRAPH

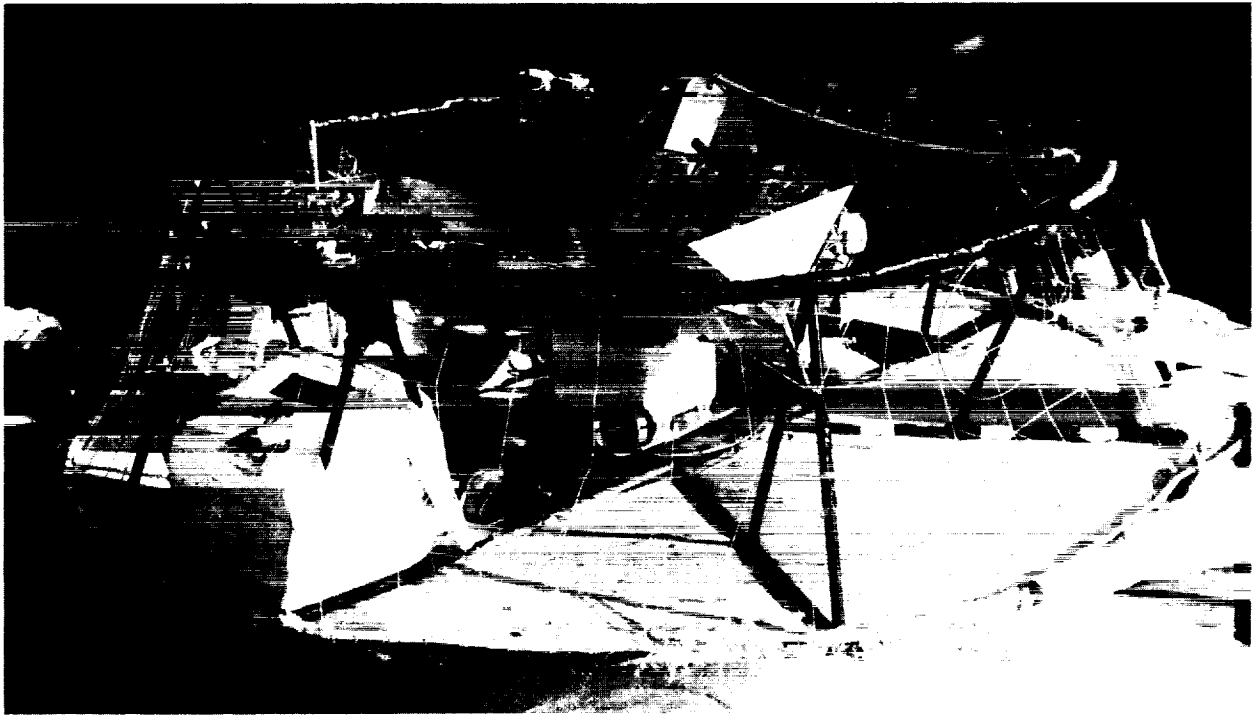


Figure 3. Aluminum Hoop Assembly with Tracker Mounted

into the top of the balloon for attaching the top payload. Two poppet valves incorporated into this mounting structure are commanded to open and release helium from the balloon at the end of the flight. The poppet valves act as a backup to the rip line.

Trying to inflate and launch a balloon with a sizeable weight attached to its top is like trying to balance a 30-ft broom handle on the end of your finger when the broom handle has a 50-lb weight on top. A tow balloon, tied to the top payload, was used during the inflation and launch phases to add stability and keep the top payload on top. This smaller balloon, about 31,000 ft³, is designed to lift about 160 lb (73 kg). The tow balloon was cut loose from the top payload after launch as soon as the main balloon stabilized and the launch-induced oscillations damped out.

3.2 TOP PAYLOAD

The top payload consists of the tracker, solar panel, voltage reference box, multiplexer, data encoder, single-frame movie camera, clock, descent parachute, and tracking beacon. All these items were mounted to the aluminum hoop assembly shown in Figure 3. The hoop assembly, with appropriately placed Styrofoam crush pads, served the following functions:

1. Permitted the top-mounted payload to "float" on top of the balloon and minimized billowing of balloon material around the top payload.
2. Served as the mounting surface to the balloon's top end fitting.
3. Provided a convenient point for attaching the tow balloon and the descent parachute.
4. Acted as a shock damper to protect and minimize damage to the top payload at touchdown.

The complete apex-mounted hoop assembly, as flown, weighed approximately 72 pounds (33 kg) and descended as a unit by parachute at flight termination.

The sun tracker, shown in Figure 3, is capable of orienting the solar panel toward the sun, compensating for the motion of the balloon by using two-axis tracking in both azimuth and elevation. The tracker has the capability to maintain its lock onto the sun to within ± 1 degree. To verify that the tracker was operating properly, the output of an on-sun indicator was constantly monitored during flight by feeding its output to the multiplexer and entering its signal into the telemetry stream. The on-sun indicator consists of a small, circular solar cell mounted at the bottom of a collimator tube, 1 in. (2.54 cm) in diameter and 4.5 in. (11.4 cm) long. The indicator was attached to the solar panel so that it pointed at the sun when the panel was perpendicular to the sun. The output of the on-sun indicator falls off very rapidly as the collimator tube points away from the sun and provides a very sensitive indication of proper tracker operation.

A reflection shield was attached to the panel to prevent any stray reflected light from reaching any of the modules. This shield was made of sheet aluminum and attached to three edges of the solar panel. The shield is the U-shaped, black object shown on the panel in Figure 3.

The solar cell modules were mounted onto the sun tracker platform with an interface of Apiezon H grease and held in place with four screws. The grease was used to achieve a highly conducting thermal contact between the modules and the panel and to smooth out the temperature distribution over the solar panel as much as possible.

The solar panel temperature was monitored using thermistors. Some of the solar cell modules were constructed with calibrated precision thermistors

embedded in the copper substrate directly beneath the solar cell. Four of these modules were mounted on the solar panel at strategic locations so their temperature readings gave an accurate representation of panel temperature. Placement of these modules on the panel is shown in Figure 2.

The PCM data encoder amplified the analog signals from the solar cells, thermistors, on-sun indicator, and reference voltages, then performed an analog-to-digital conversion. The encoder had a programmable control unit that was used to set bit rate, bits per word, parity, analog-to-digital conversion, and format. A PROM was used to provide format control. Four 32-channel multiplexers allow sampling of up to 128 data channels and amplify the low-level signals from the experimental package. The amplifier was designed to process voltage signals at input levels up to 100 mV. The multiplexer stepped through the various channels at a rate of two scans per second, i.e., every data channel is read twice each second.

An ultrawide angle, single-frame movie camera mounted at the perimeter of the aluminum hoop provided visual documentation of tracker operation. A battery-powered timer activated the shutter at 10-second intervals, so that 50 ft of 8-mm movie film is sufficient to record the entire flight from launch to landing. A wind-up clock was placed in the camera's field of view for correlation of tracker operation to the telemetered data. The pictures provide a complete record of ascent, tracker operation at float altitude, descent, touchdown, and post-touchdown events.

A tracking beacon, like those used to track wild turkeys in their native habitat, was used this year on a trial basis. This beacon, which transmits in the 160 MHz range, was attached to the hoop assembly and proved to be very

useful in finding the payload during the recovery stage of the flight. It is planned to incorporate a similar beacon on all future flights.

3.3 BOTTOM PAYLOAD

The bottom payload was entirely furnished by the NSBF. It consists of a battery power supply, a ballast module for balloon control, and an electronics module known as the Consolidated Instrument Package (CIP).

Power for operating most of the electrical and electronic equipment on the balloon was supplied by a high-capacity complement of lithium batteries. This supply, furnishing 28 VDC regulated power and 36 VDC unregulated power, powered the sun tracker and all the instruments in the CIP. Several other small battery sources were used at various locations on the balloon for instruments that require small amounts of power. For example, the tracking beacons, the voltage reference box, and the camera timer all had individual battery power supplies. All batteries were sized to supply power for at least twice the expected duration of a normal flight.

High-altitude balloons tend to lose helium slowly during the course of the flight. As a consequence, a helium balloon will tend to reach float altitude and then begin a slow descent. To counteract this tendency, a ballast system was included as part of the bottom payload. It contained approximately 150 pounds (68 kg) of ballast in the form of very fine steel shot. The shot may be released in any desired amount by radio command. By proper use of this system, float altitude may be maintained to within $\pm 2,000$ ft (± 600 m).

The telemetry system was contained in the CIP. A block diagram of the telemetry system is shown in Figure 4. The system sent all data transmissions

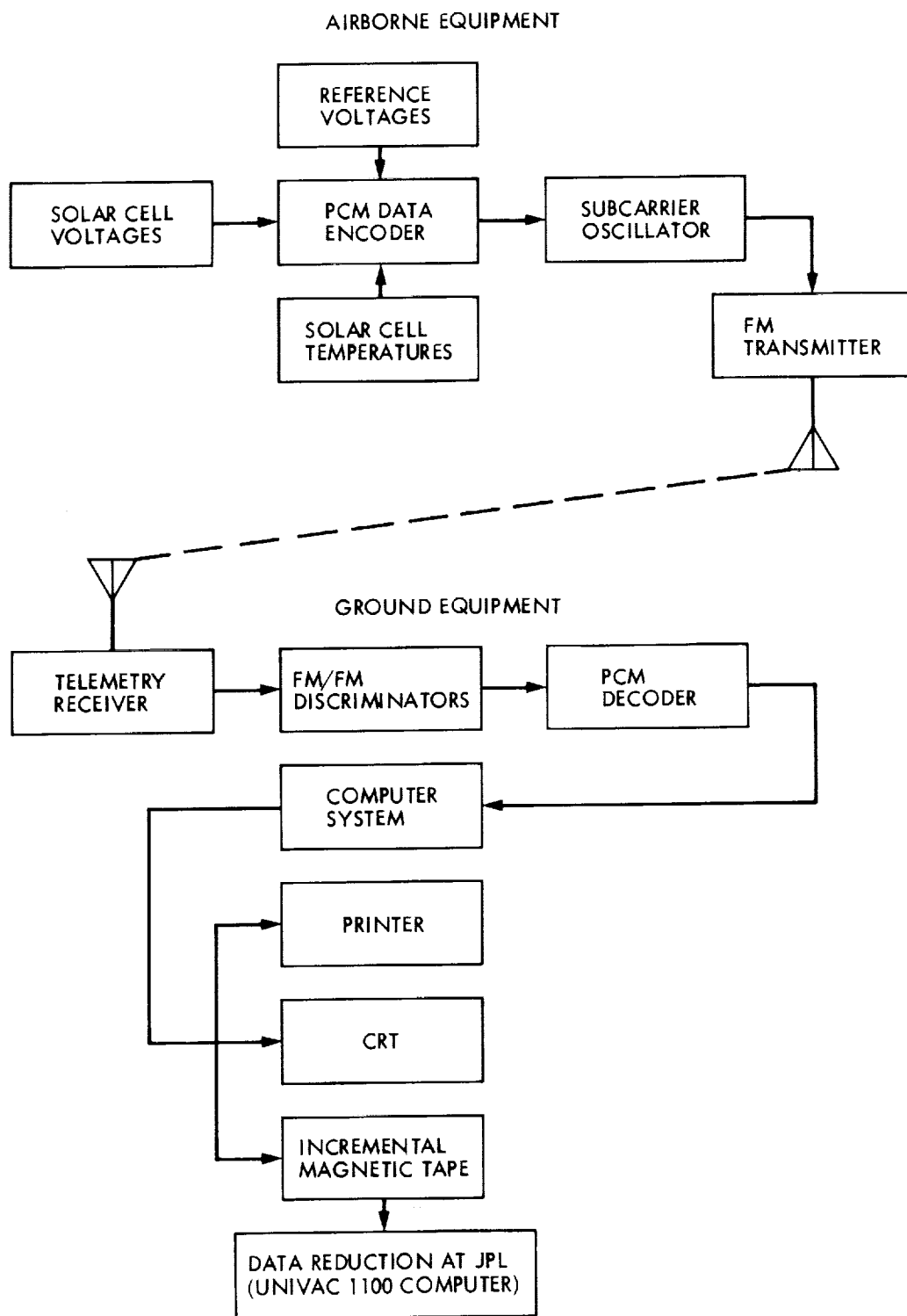


Figure 4. Block Diagram of Balloon Telemetry System

concerning the flight over a common RF carrier. The CIP also contained a command system for sending commands to the balloon for controlling scientific payloads or for controlling the housekeeping functions on the balloon.

Specifically, the CIP contained the following equipment:

1. MKS pressure transducers
2. Omega receiver
3. Subcarrier oscillators as required
4. L-band FM transmitter
5. High-frequency tracking beacon transmitter
6. Transponder for air traffic control tracking
7. PCM command receiver-decoder
8. Loran receiver

The altitude of the balloon was measured with a capacitance-type electronic transducer, which read pressure within the range of 1020 to 0.4 millibars (102,000 to 40 Newtons/m²) with an accuracy of 0.05%. The transducer produced a DC level that was encoded as PCM data and decoded at the receiving station into pressure, and then the altitude was calculated from the pressure reading.

The Omega and Loran navigation systems were used for flight tracking. An onboard receiver was used to receive these signals for retransmission to the processor in the ground station. This system can provide position data to an uncertainty of less than 2 mi (3.2 km). The Loran signal was multiplexed into the telemetry stream and updated every 8 seconds.

As previously mentioned, all the telemetry data was sent to the ground in the form of pulse code modulation. A UHF L-band transmitter in the CIP was

used to generate the RF carrier. The L-band carrier was modulated by the pulse code and sent to the receiving station at Palestine.

Several tracking beacons were used on the balloon. A low-frequency transmitting beacon, attached to the lower payload, was used by the automatic direction finding (ADF) system in the recovery airplane to track and locate the balloon during flight and recovery. An aircraft type transponder was flown so that Air Traffic Control could read the balloon's location on their radar systems during the flight.

The purpose of the PCM command system is to send commands to the balloon, i.e., to turn the tracker on or off, terminate the flight, etc. It was designed to reject false commands and was highly reliable in operation. The data was encoded on a frequency-shift-keyed audio carrier. This signal was then decoded into data and timing control. Each command consisted of a double transmission of the data word. Both words must be decoded and pass a bit-by-bit comparison before a command is executed. Commands may be sent to the balloon from either the ground station at Palestine or from the recovery airplane.

The lower payload is suspended from the balloon by a 8.5-m-diameter parachute. The top end of the parachute was fastened to the bottom of the balloon and the lower payload, containing the CIP, the battery power supply, and the ballast, was attached to the shroud lines. Appropriate electrical cables and break-away connectors were rigged in parallel with the mechanical connections. The whole bottom assembly was designed to break away from the balloon and fall to earth suspended from the parachute at termination of the flight.

4. FLIGHT SEQUENCE

4.1 PRELAUNCH PREPARATIONS

The balloon launching pad at the NSBF is a large circular area, 2,000 ft (600 m) in diameter. In the center of this large circle is another circular area, solidly paved, measuring 1,000 ft (300 m) in diameter. Grass is planted in the area between the two circles, and a paved road surrounds the large circle. Paved radials extend from the perimeter road toward the launch pad.

When all prelaunch preparations had been completed and the staff meteorologist had predicted favorable weather and winds at Palestine and for some 300 mi (480 km) down range, the equipment was taken to the launch site. The main balloon, protected by a plastic sheath, was laid out full length on the circular paved area. It was aligned with the direction of the wind, with the top of the balloon upwind. The top end of the balloon was passed under, behind, and over the top of a large, smooth, horizontal spool mounted on the front end of the spool vehicle. One end of this launching spool was hinged to the spool vehicle. The other end of the spool had a latch that could be released by a trigger mechanism. After the balloon was passed over the spool, the spool was pushed back to engage the latch so that the spool trapped the balloon. The top 10 m or so of the balloon was pulled forward from the spool, allowing the top payload to rest on the ground. It is this top 10 m of balloon that later receives the helium gas during inflation. The helium forms a kind of bubble in this part of the balloon above the launching spool. After the launching spool was latched, final preparations of the top payload were begun. The tow balloon was attached to the hoop with nylon lines, the clock

was wound, the camera was energized, and a final checkout of the tracker and data encoder was performed.

Preparations at the bottom end of the balloon proceeded in parallel. The balloon was connected to the top center of the parachute canopy, and the parachute's shroud lines were connected to the bottom payload using a special fitting. All the connecting wires, lines, and cables associated with the bottom payload cables were passed up and over a high, platform-like structure on the top of the launch vehicle. On the forward part of this structure, a fixed pin pointed forward. A hole in the special shroud-line fitting was passed over this pin, and a quick-release mechanism latched the fitting to the pin. The lower payload was thus suspended from the pin in front of the vehicle in full view of the vehicle's driver. After completion of all the mechanical and electrical hookups at both top and bottom payloads, a final checkout of all the CIP and ballast systems was performed.

The launch sequence began by inflating the tow balloon with helium. The main balloon was then inflated by passing a predetermined volume of helium through two long fill-tubes and into the balloon as shown in Figure 5. The balloon was launched by triggering the latch on the launching spool. When the latch released, a stout spring caused the free end of the spool to fly forward, rotating about the hinge. This released the balloon. As the balloon rose, the launch vehicle at the lower end of the balloon began to move forward (downwind). When the driver of the launch vehicle had positioned the vehicle directly below the balloon and had his vehicle going along at the same speed as the balloon, he released the latch on the pin and the lower payload was released. Figure 6 shows the balloon system and the launch vehicle a few seconds after release of the launching spool just as the downwind launch

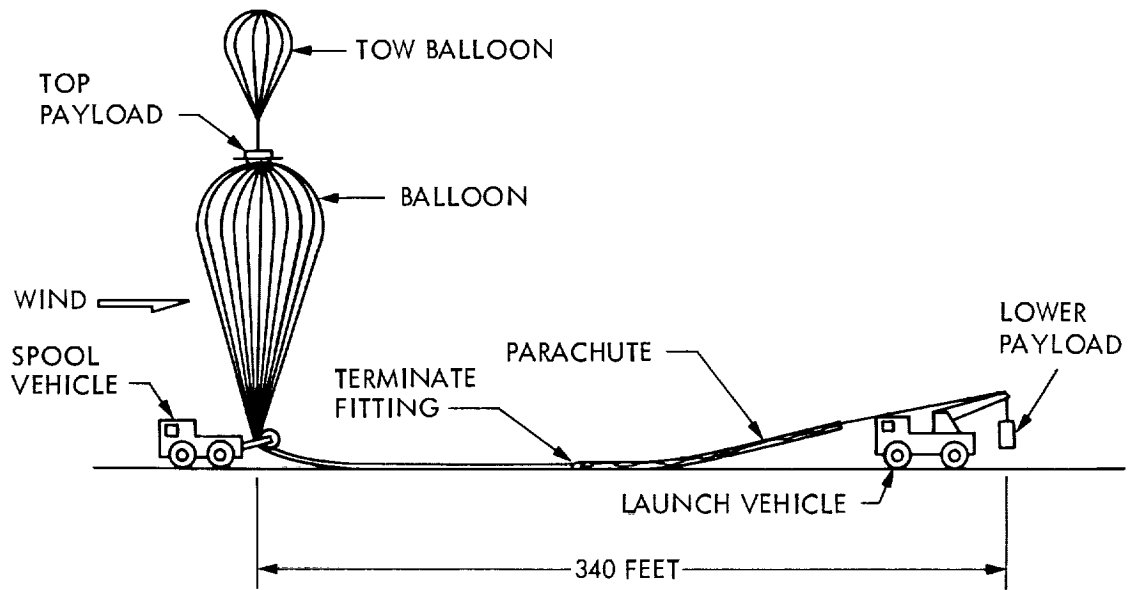
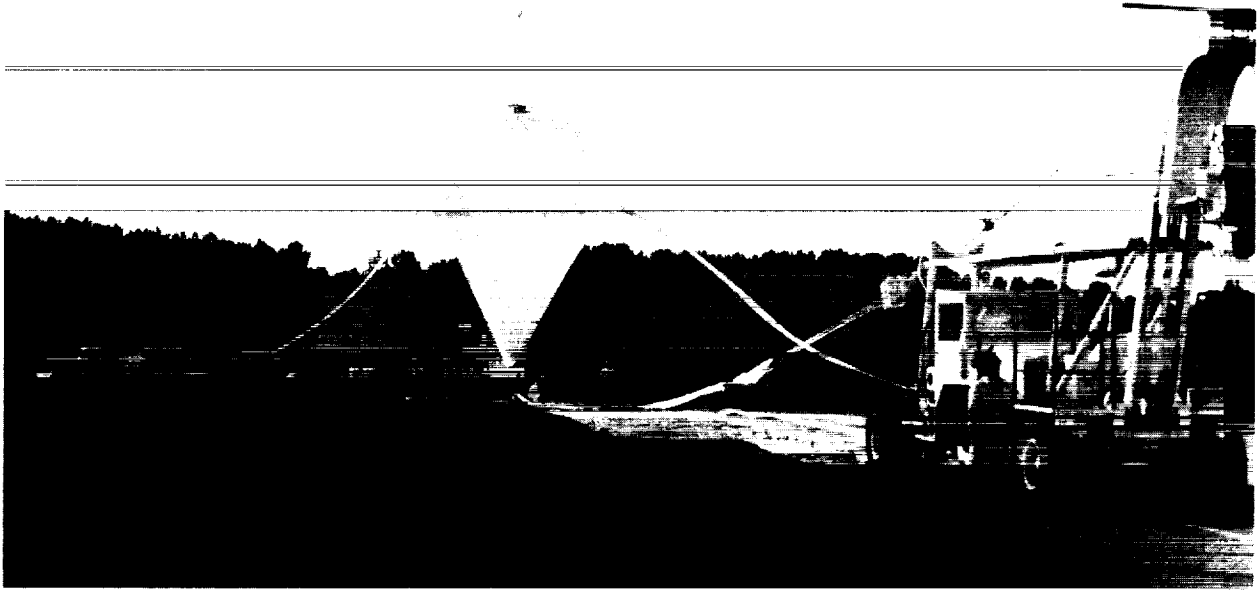


Figure 5. Flight Train Configuration

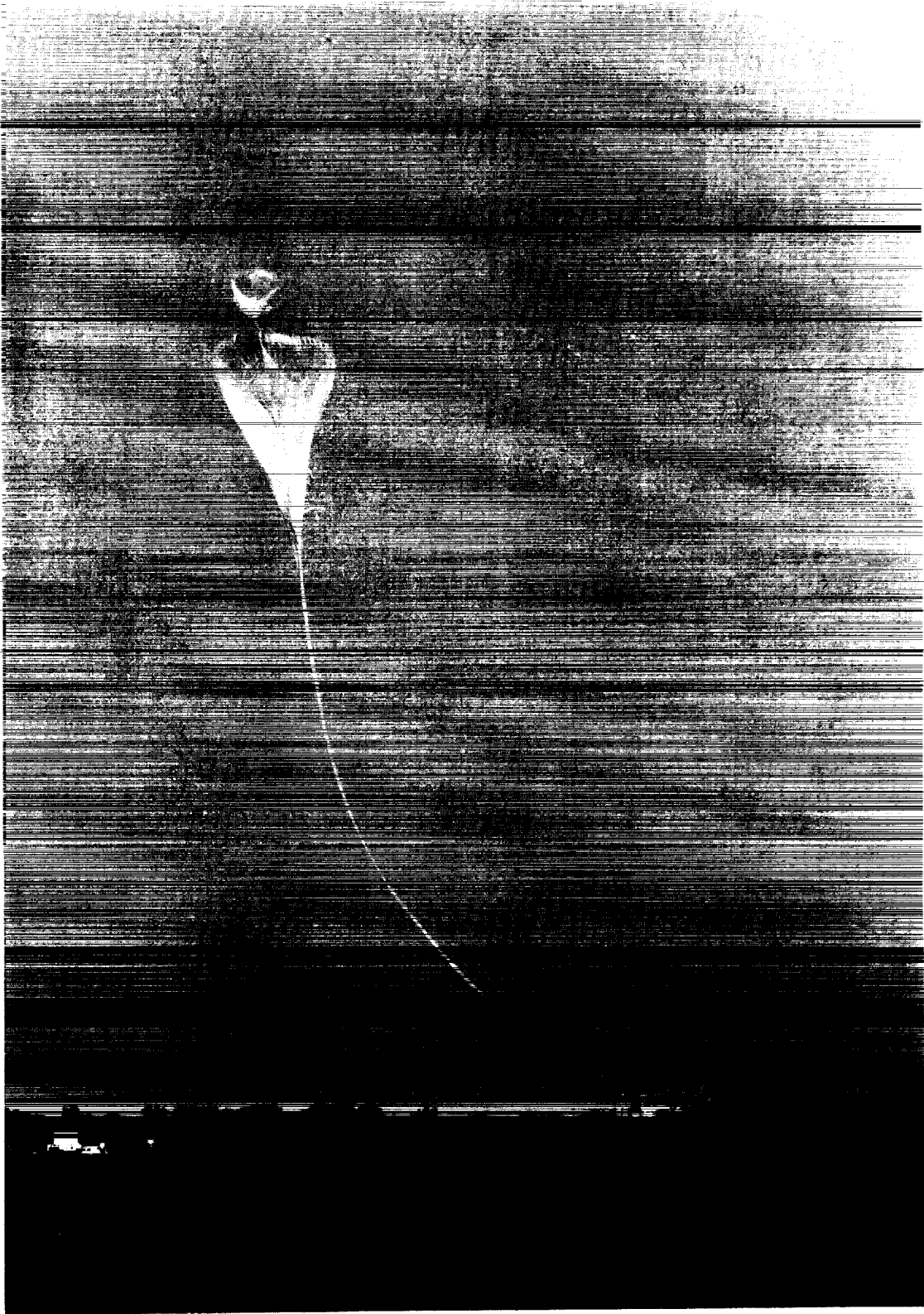


Figure 6. Balloon Launch

vehicle began to move. As soon as the main balloon quit oscillating, a signal was sent from the launch pad triggering an explosive charge. This released the tow balloon and the launch sequence was complete.

4.2 FLIGHT

The balloon ascended at a rate of approximately 1000 ft/min (5.0 m/s) and reached float altitude after approximately 2 hours. During the ascent, the flight controller at Palestine maintained a constant contact with Air Traffic Control (ATC). Data from the onboard navigational system was continuously given to ATC so that air traffic in the area could be vectored around the balloon.

After the balloon had been launched, solar cell voltages, interspersed with reference calibration voltages and thermistor voltages, were fed into the telemetry system. These voltages were converted to PCM and were transmitted to the NSBF ground station along with the navigational, altitude, and other information from the CIP. At the ground station they were decoded, recorded, and displayed in real time for monitoring of the flight. The flight was timed to reach float altitude approximately 3 hours before solar noon, and the tracker was turned on by telemetry command prior to reaching float altitude as the balloon ascended 80,000 ft. Tracker operation was monitored by observing the telemetered values for the current drawn by the tracker motors, the output of the on-sun indicator, and the outputs of about half the solar cell modules. Data was recorded from 1700 GMT through 1940 GMT when the flight was terminated. Solar noon occurred at approximately 1830 GMT for this flight.

4.3 FLIGHT TERMINATION

Shortly after launch and while the balloon was ascending, the recovery airplane took off from Palestine with the recovery crew aboard. This airplane was equipped with a radio system that allowed the crew to maintain constant communication with the balloon base either by direct transmission or by radio relay from the balloon. The airplane also had a full command system so that it could send commands to the balloon. During the summer months, the winds at altitudes above 80,000 ft (24 km) blow from east to west at speeds of about 50 knots (25 m/sec), so the airplane had to fly about 300 mi (180 km) west of Palestine to be in position for recovery. The pilot can fly directly toward the balloon at any time by using the ADF to track the low-frequency beacon. The pilot of the recovery airplane is responsible for the termination phase. Before leaving Palestine, the pilot had been provided a set of descent vectors by the staff meteorologist. The descent vectors are an estimate of the trajectories the payloads will follow as they come down on their parachutes. Upon receiving word from Palestine that the experimenter had all the data he needed, the pilot flew under the balloon and established its position accurately by visual observation. Using the descent vectors, he then plotted where the payloads should come down. He also established contact with Air Traffic Control. When ATC advised that the payloads would not endanger air traffic, and when the descent vector plots showed that the payloads would not come down in an inhabited area, the pilot sent the commands to the balloon for termination of the flight.

The termination sequence consisted of first sending a command that disconnected power from the tracker and data encoder. Next a command was sent

that cut the electrical cable running from the bottom payload to the top payload. This command simultaneously cut the cables holding the top payload onto the top of the balloon and opened the poppet valves on the top of the balloon. A second command released the bottom parachute from the balloon, allowing the bottom payload to fall away and caused the balloon to become top heavy. As the bottom payload fell, a ripcord attached to the top of the parachute opened a large section in the balloon. The balloon collapsed, the top payload fell off the balloon, its parachute opened and all three objects began their descent.

Approximately 1 hour is required for the two parachutes and the balloon to fall from float altitude at the descent rate of roughly 1250 ft/min (6.4 m/s). During this time, the pilot monitored the position of the bottom payload using his ADF. He also monitored the altitude information from the pressure transducer and relayed this information along to ATC. After reaching the ground, all three items had to be found. The beacons on the top and bottom payloads usually aid in locating them rather quickly. Search patterns centered on the impact zones calculated from the descent vectors are flown as necessary. Once the impact locations were established from the air, the ground recovery crew was directed into the proper areas to recover the payloads.

Figure 7 is the flight profile for the 1989 balloon flight (No. 1486P in the nomenclature of the NSBF). The plot shows altitude vs distance from the launch site from the time of launch until touchdown. The points are plotted on approximately 10-minute time intervals. As the figure shows, the touchdown site was approximately 235 mi (480 km) from the launch site and the total flight duration was about 5 1/2 hours.

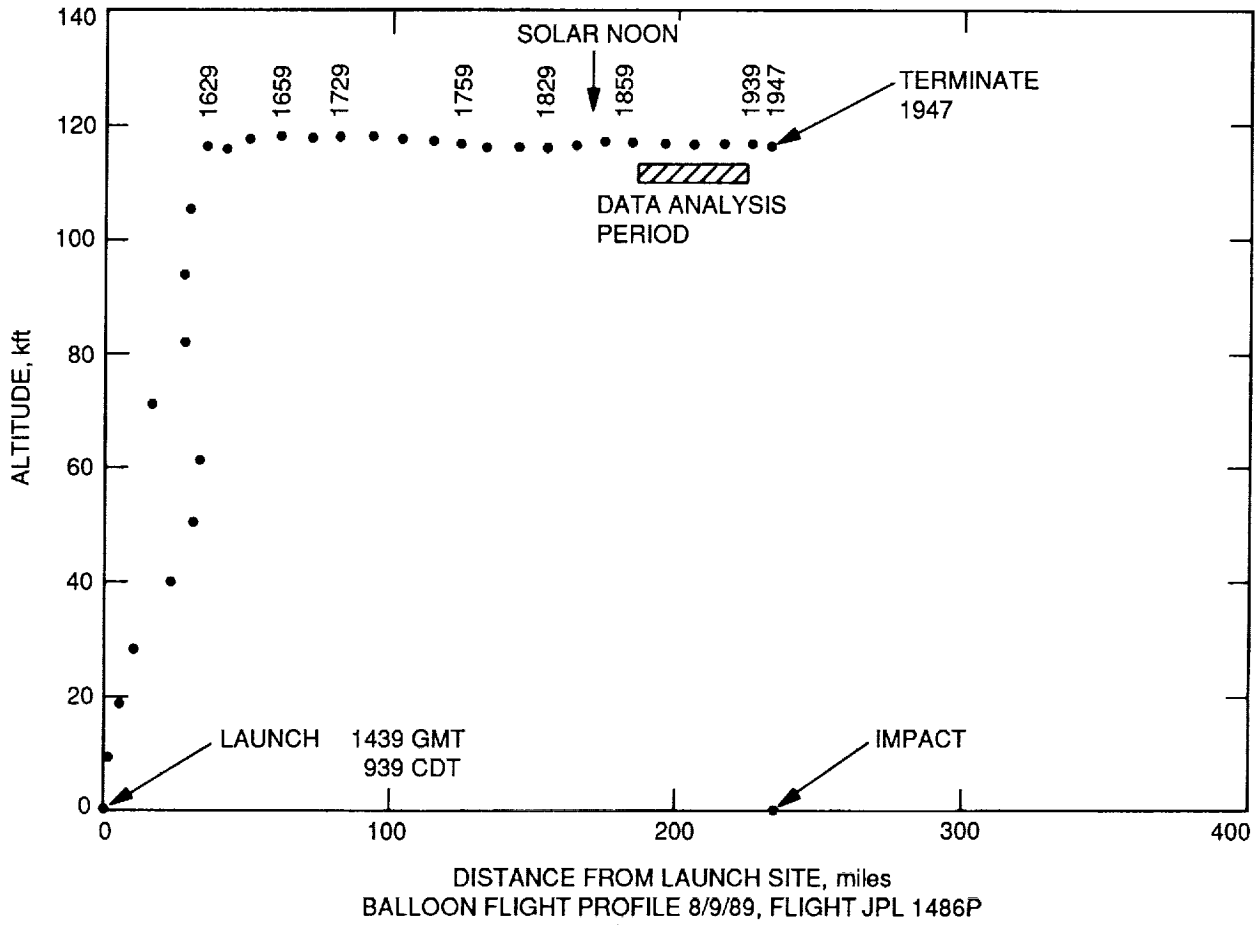


Figure 7. 1989 Balloon Flight Profile

5. DATA ANALYSIS

The computer analysis was performed at JPL using the Univac 1100 computer. The program read the raw data from the magnetic tape produced during the flight, then corrected the cell data for temperature and sun-earth distance according to the formula:

$$V_{28,1} = V_{T,R}(R^2) - A(T - 28)$$

where

$V_{T,R}$ = measured module output voltage at temperature T and distance R.

R = sun-earth distance in astronomical units (AU).

A = module output temperature coefficient.

T = module temperature in degrees C.

The remainder of this section describes the details of performing the above corrections and computing calibration values for the cells.

5.1 COMPUTER ANALYSIS

The computer program read data from the magnetic tape one record at a time. Each record contained 16 scans of data plus a ground frame. Each scan of data consisted of two synch words followed by a reading of each of the 64 data channels. The ground frame contained the date and time of the scan, followed by the latitude, longitude, and pressure as measured by instruments on the balloon. The program first checked the ground frame to see whether the record fell within the allowed data analysis time. (The allowed data analysis time window is an input to the program set by the parameters MINTIM and MAXTIM). The computer rejected the entire frame if the time of the current record fell outside the time window or if it could not read the time properly.

The computer read records within the time window until it had accumulated 200 scans. Each set of 200 scans is called a pass. At this point, the data was in pulse code modulation (PCM) counts. The PCM data for each channel was averaged, then a screening procedure was used to reject scans containing questionable data. For example, scans were rejected if the on-sun indicator was lower than a threshold value (input parameter OSMIN). Scans were also rejected if the PCM count for a data channel was not within the allowable PCM count range, if there was too large a count deviation on any channel from one scan to the next, or if there was an unrecoverable problem in reading the tape.

The PCM data was next converted to engineering units. The program has a provision for doing this in any of four different ways. The simplest and most commonly used method will be described here. During the calibration of the telemetry system, the output of the telemetry system vs the input from the voltage reference box was recorded to produce a table of mV input vs PCM count output. Similarly for the thermistor channels, a series of resistors was connected one by one across a thermistor channel and the resulting PCM count for that channel recorded. Since the temperature corresponding to each resistance value was known, the construction of a PCM count vs temperature table was possible. This procedure was repeated for all thermistor channels and a calibration table was constructed for each thermistor channel. All these calibration values were input to the computer program. During conversion of solar cell data to mV, the computer performed a linear interpolation in the PCM vs mV table. At the completion of the initial computer analysis run, the output values of each channel corresponding to voltage reference levels were checked. If they were found to have held

constant during the flight (they normally read constant to within \pm one PCM count out of 1,000) the use of the simple linear interpolation scheme was continued for the final data analysis. Since the relationship between thermistor resistance vs temperature is nonlinear, a third degree polynomial was used for the interpolation of the temperature values.

At the end of each pass, four averages were computed for each channel: (1) an initial average based on all acceptable scans, (2) a corrected average, using all data falling within a specified fractional deviation (input parameter ADEV) of the initial averages, (3) the corrected average multiplied by the square of the earth-sun radius vector (in AU) for the day of the flight (input parameter RV), and (4) a final average with all the above corrections plus a temperature correction to 28°C. This final correction used the values of the temperature coefficients measured in the laboratory (input parameters TPCOEF).

As Figure 1 shows, about half the panel area was populated with modules painted black. The other half of the panel had modules painted white. The left half of the panel reached an average temperature of 80°C during the flight, while the right half ran at 74°C. Therefore, the analysis program was run twice, once for the six large black modules using temperature sensors T1 and T2, then rerun for the remaining 36 cells on the right side of the panel using temperature sensors T3 and T4.

This completes the data analysis for one pass of data. The entire process was repeated by returning to the tape-reading routine and reading another pass (200 scans) of data. All the screening and averaging routines were performed on this pass also, and this procedure was continued until 5 passes of data had been analyzed or until MAXTIM was exceeded.

In addition to the averages taken after each pass, an overall summary matrix was constructed which contained the fully corrected averages for each channel after each pass. A row of entries was added to this matrix after each pass. After all passes had been completed, an overall average and standard deviation were computed for each channel. These overall averages of approximately 1000 readings are the reported calibration values for the modules.

5.2 CALIBRATION RESULTS

Table 1 reports the calibration values of all the cells calibrated on the 1989 balloon flight, corrected to 28°C and to 1 AU. The table also reports the standard deviation of the 1,000 measurements, the preflight and postflight readings of each module in the X25 simulator, a comparison of the preflight with the postflight simulator readings, and a comparison of the preflight simulator readings with the balloon calibration readings. The table also reports the temperature coefficients measured for each module in the laboratory.

5.3 UPDATE OF BFS-17A DATA

Several standard modules have been flown repeatedly over the 25-year period of calibration flights. The record of the one with the longest history, BFS-17A, appears in Table 2 along with some computed statistical parameters. The standard deviation of 0.28 (0.46%) and a maximum deviation of 0.74 (1.23%) from the mean show that the BFS-17A readings are very tightly grouped. In addition to giving a measure of the consistency of the year-to-year measurements, BFS-17A also provides some insight into the quality of the solar irradiance falling on the solar panel with regard to uniformity,

shadowing, or reflections. Since this cell has been mounted in various locations on the panel over the years and its readings have been quite consistent, there does not seem to be any evidence of nonuniformity over the panel.

Table 1. 1989 Balloon Flight 8/9/89 118,000 ft RV=1.0136862 Flight No. 1486P

MODULE NUMBER	CODE	TEMP. INTENSITY ADJUSTED AVERAGE	STANDARD DEV.	PRE-FLT POS-FLT AMPO, SOLAR SIM. 1AU, 28°		COMPARISON, SOLAR SIMULATOR & FLT		TEMP. COEFF. (mV/C)	COMMENTS
				PRE-FLT	POS-FLT	PRE-FLT VS. POS-FLT (PERCENT)	FLIGHT VS. PRE-FLT (PERCENT)		
89-141	ASEC	80.59	.09839	79.01	79.01	.00	2.52	.0750	Space Stn 8X8
89-142	ASEC	81.23	.12335	79.33	79.41	.10	2.82	.0767	Space Stn 8X8 T2
89-143	ASEC	80.47	.05397	79.06	79.16	.13	2.37	.0763	Space Stn 8X8
87-143	BOEING	48.15	.02033	54.79	54.91	.22	-12.16	-.0349	CIS, AlGaAs filter
89-151	BOEING	23.92	.06019	28.16	27.89	-.96	-14.91	.0076	GaSb
89-154A	BOEING	65.00	.19789	59.59	59.61	.03	9.05	.0593	GaAs
89-154B	BOEING	52.03	.18586	59.72	59.45	-.45	-12.82	-.0948	CIS
89-131	FORD	73.81	.04311	74.12	73.97	-.20	-.41	.0469	AEG 2 Ohm BSR
78-110	HUGHES	97.33	.31736	95.41	95.41	.00	1.91	.0501	K7 Refly
89-1710	HUGHES	61.96	.03209	57.26	57.33	.12	8.18	.0496	GaAs/Ge
86-023	JPL	58.30	.03779	54.19	54.69	.92	7.60	.0591	GaAs Mantech T3
88-004	JPL	59.71	.03023	55.93	55.75	-.32	6.84	.0572	GaAs/Ge
89-001	JPL	14.70	.10405	59.41	22.34	62.40	-75.09	-.1609	CIS
89-002	JPL	61.86	.03175	60.43	60.33	-.17	2.32	.0450	InP
89-003	JPL	61.02	.02790	60.19	59.95	-.40	1.45	.0528	InP
89-005	JPL	60.36	.04515	56.01	56.02	.02	7.77	.0571	GaAs/Ge
89-006	JPL	59.78	.16904	55.27	55.01	-.47	8.10	.0551	GaAs/Ge
89-007	JPL	60.04	.15424	55.57	55.30	-.49	8.02	.0578	GaAs/Ge
89-008	JPL	59.73	.02981	55.42	55.31	-.20	7.84	.0547	GaAs/Ge
BFS-17A	JPL	59.62	.03604	60.25	60.07	-.30	-1.02	.0354	Standard
89-101	SATO	62.40	.03350	57.91	57.99	.14	7.77	.0475	GaAs/Si
89-102	SATO	64.35	.17175	58.79	58.73	-.10	9.33	.0473	GaAs/Si
89-103	SATO	62.34	.02925	57.38	57.48	.17	8.65	.0460	GaAs/Si
89-111	SOLAREX	88.36	.06099	89.87	89.87	.00	-1.66	.0566	Si Textured
89-113	SOLAREX	80.04	.18562	80.04	80.26	.27	-.10	.0526	Si 2 mil boron
89-121	SOLAREX	77.07	.09997	75.99	75.62	-.49	1.77	.0600	Space Stn 8X8 T1
89-123	SPECTROLAB	77.78	.04064	77.34	76.08	-1.63	1.07	.0652	Space Stn 8X8
89-125	SPECTROLAB	77.02	.06736	76.72	75.95	-1.00	.84	.0717	Space Stn 8X8
89-127	SPECTROLAB	77.33	.09608	30.72	30.72	.00	-10.94	-.0948	Ge Cell/GaAs Filter
87-196	TRW	88.95	.27767	83.05	77.77	-6.36	7.24	.0415	Concentrator T4
89-181	TRW	65.51	.05756	60.49	60.34	-.25	8.26	.0596	GaAs
89-184	TRW	57.52	.19686	52.06	52.20	.27	10.34	.0375	GaAs
85-111	VARIAN	62.61	.05229	57.62	57.96	.59	8.65	.0495	GaAs Refly
87-204	VARIAN	19.90	.01869	17.44	17.48	.23	14.16	.0119	1.93 eV AlGaAs Refly
89-161	VARIAN	31.74	.09397	27.40	27.37	-.11	15.61	.0224	1.93 eV AlGaAs
89-164	VARIAN	29.31	.04750	29.10	29.17	.24	.93	.0375	AlGaAs/GaAs
89-165	VARIAN	29.80	.08333	29.64	29.67	.10	.53	.0422	AlGaAs/GaAs
89-171	VARIAN	63.86	.10294	59.33	59.41	.13	7.53	.0569	GaAs
89-172	VARIAN	29.49	.06195	60.38	31.35	48.08	-51.05	.0556	GaAs
89-191	WPAFB	55.36	.13126	61.72	62.55	1.34	-10.06	-.2189	Ge/GaAs Window
89-192	WPAFB	54.60	.16806	61.10	61.95	1.39	-10.31	-.2167	Ge/GaAs Window
89-193	WPAFB	27.96	.06250	30.20	29.90	-.99	-7.55	-.1983	Thin Al/Ga/As
0MV		.00*	.00000	.00	.00	.00	.00	.0000	
100MV		99.94*	.04854	.00	.00	.00	.00	.0000	
80MV		79.79*	.00620	.00	.00	.00	.00	.0000	
50MV		50.00*	.00000	.00	.00	.00	.00	.0000	

Table 2. Repeatability of Standard Solar Cell BFS-17A
(41 Flights Over a 27-year Period)

Flight Date	Calibration Value, mV	Flight Date	Calibration Value, mV
9/ 5/63	60.07	4/ 5/74	60.37
8/ 3/64	60.43	4/23/74	60.37
8/ 8/64	60.17	5/ 8/74	60.36
7/28/65	59.90	10/12/74	60.80
8/ 9/65	59.90	10/24/74	60.56
8/13/65	59.93	6/ 6/75	60.20
7/29/65	60.67	6/27/75	60.21
8/ 4/66	60.25	6/10/77	60.35
8/12/66	60.15	8/11/77	60.46
8/26/66	60.02	7/20/78	60.49
7/14/67	60.06	8/ 8/79	60.14
7/25/67	60.02	7/24/80	60.05
8/ 4/67	59.83	7/25/81	60.07
8/10/67	60.02	7/21/82	59.86
7/19/68	60.31	7/12/83	60.10
7/29/68	60.20	7/19/84	59.84
8/26/69	60.37	7/12/85	59.99
9/ 8/69	60.17	7/15/86	59.44
7/28/70	60.42	8/23/87	60.63
8/ 5/70	60.32	8/ 7/88	60.24
		8/ 9/89	59.62
	Mean	60.180	
	Standard Deviation	0.278	
	Maximum Deviation	0.740	

9/5/63 to 8/5/70 Each data point is an average of 20 to 30 points per flight

4/5/74 to 7/1/75 Each data point is an average of 100 or more points per flight

6/10/77 to 7/21/82 Each data point is an average of 200 data points

7/12/83 to 8/7/88 Each data point is an average of 4000 data points

8/9/89 Each data point is an average of 1000 data points

6. CONCLUSIONS

The 1989 balloon flight was a successful flight. BFS-17A again returned readings that are nearly identical to the readings returned on the previous 40 flights. In addition to BFS-17A, four cells from previous flights were reflowed this year. One GaAs on Ge cell (No. 88-004), one GaAs cell (No. 85-111), one 1.93 eV AlGaAs cell (No. 87-204), and one Si cell (No. 78-110) were reflowed in 1989. The GaAs/Ge cell measured 59.71 mV, which is 1.38% below its calibration value determined in 1988. The GaAs cell measured 62.61 mV, 0.84% below its 1985 calibration value. The AlGaAs cell decreased from 20.65 mV measured in 1987 to 19.90 mV in 1989, a 3.63% decrease. The Si cell measured 97.33 mV, which is 0.92% above its original calibration value of 96.44 mV measured in 1978 and 1.25% above its most recent calibration value of 96.12 mV measured in 1987. With the exception of the AlGaAs cell, the reflowed cells deviated no more than 1.4% from their previous readings.

7. REFERENCE

B.E. Anspaugh, R.G. Downing and L.B. Sidwell, Solar Cell Calibration Facility Validation of Balloon Flight Data: A Comparison of Shuttle and Balloon flight Results, JPL Publication No.85-78, Jet Propulsion Laboratory, Pasadena, Calif., October 15, 1985.

